Energies of sp^2 carbon shapes with pentagonal disclinations and elasticity theory

Energies of sp^2 carbon shapes with pentagonal disclinations and elasticity theory

Antonio Šiber

Institute of Physics, PO Box 304, 10001 Zagreb, Croatia

E-mail: asiber@ifs.hr

Abstract
Energies of a certain class of fullerene molecules (elongated, contracted and
regular icosahedral fullerenes) are numerically calculated using a
microscopic description of carbon–carbon bonding. It is shown how these
results can be interpreted and comprehended using the theory of elasticity
that describes bending of a graphene plane. Detailed studies of a wide variety
of structures constructed by application of the same general principle are
performed, and analytical expressions for energies of such structures are
derived. Comparison of numerical results with the predictions of a simple
implementation of elasticity theory confirms the usefulness of the latter
approach.

(Some figures in this article are in colour only in the electronic version)

1. Introduction

Recent years have been marked by an accented interest of scientists in molecules and materials made exclusively of carbon atoms (C). This interest has been initiated by discoveries of fullerenes [1] and carbon nanotubes [2], and is fuelled by many different nanoscopic shapes and structures made of carbon atoms that are continually appearing either as a result of experimental studies [3–5] or imaginative theoretical constructions [6–9]. Structures of interest to this work are those in which carbon atoms are sp^2 hybridized, as in the graphene layers in graphite. Fullerenes and carbon nanotubes fit in this category, but there are many other different shapes and objects that can be constructed. The multitude of possible shapes is a result of pronounced anisotropy of carbon–carbon interactions and the relatively low energy needed to transform a hexagonal carbon ring into a pentagonal one. Inclusion of heptagonal rings allows for the creation of additional, negative-Gaussian-curvature shapes [9] that are not a subject of this paper. Carbon shapes are of interest since the same elementary constituents (sp^2 hybridized carbon atoms) can be 'assembled' in a variety of stable shapes that will not spontaneously decay or transform into other shapes once created. The resulting shapes and structures may differ in their functionality, whatever their purpose may be. The assembly of simple elementary pieces into a possibly 'engineered' or 'designed' shape is a dream of nanotechnologists, and the carbon structures are thus the ideal benchmark system. Nanoscale shapes of biological interest are often self-assembled—a prime example is the self-assembly of viral coatings from individual proteins that make them [10]. Even more intriguingly, the symmetries and shapes of icosahedral viruses are directly related to symmetries of 'gigantic' fullerenes [11–13]. Both types of structures are characterized by pentagonal 'disclinations' [14] (pentagonal carbon rings in fullerenes [11] versus pentameric protein aggregates in viruses [15]) in crystalline sheet, and both can be constructed from the triangulation of an icosahedron. This may be a coincidence, but may also point to more general and fundamental principles that may still be discovered in the study of carbon structures and shapes. Viruses, as carbon shapes, also show the property of multiformity. The same viral coating proteins may assemble in icosahedral shells of varying symmetry, but may also make spherocylindrical or conical particles or even protein sheets, depending on the conditions [13, 15]. Similar features are found in sp^2 carbon shapes. Although various shapes can be, more or less easily, imagined, this does not mean that they should have large

binding energies, or that they should be bound at all. Therefore, it seems pragmatic to have a rule of thumb estimate for their energy, based solely on their imagined shape. The theory of elasticity provides an excellent framework for such estimates and has been in the past successfully applied for this purpose [12, 13, 16, 17]. The aim of this paper is to show how the energies of the various shapes that can be imagined may be estimated from simple relationships that are quite accurate when applied properly. In certain aspects, this paper is a continuation of efforts started in [16] and [17], but differs from them in that it studies a certain class of convex carbon shapes that include both capped carbon nanotubes and fullerenes as special limiting cases. It also applies the theory of elasticity in more difficult circumstances in which the symmetry of shapes is reduced.

In section 2 I shall present the geometric construction of a certain class of shapes that is of interest to this paper. In section 3 I shall describe the procedure that is used to find minimal energy shapes based on the geometric construction discussed in section 2. The procedure is based on the implementation of the conjugate gradient technique [21] in combination with the latest Brenner's potential for the description of carbon–carbon bonding [22], which provides an excellent opportunity to further examine the predictions of this relatively recently proposed potential, although the main message of this paper is totally independent on the form of the potential used. Section 4 contains numerical results of this paper, together with elements of elasticity theory that are applied in the analysis of these results. It will be demonstrated how a simple characterization of the graphene elasticity together with the knowledge of the energy for creation of pentagonal disclination enables a reliable estimate of energies of various convex shapes. Section 5 summarizes and concludes the paper.

2. Construction of shapes of interest

The shapes of interest to this work can be constructed as depicted in figure 1. The procedure is to cut out the outlined shape from the graphene plane and fold it into a polyhedron. The shapes that shall be considered can be loosely termed as elongated, regular or contracted icosahedra. Note that the construction results in 12 pentagonal carbon rings situated in vertices of (contracted or elongated) icosahedron. The equilibrated, minimal energy shapes obtained from the pieces of cut-out graphene plane are also displayed in figure 1. The numerical procedure that was used to obtain these shapes will be discussed in detail in section 3. At this point, note that the elongated shapes resemble carbon nanotubes, while the highly contracted shapes look almost like two cones glued together at their bases—there are two pentagonal carbon rings at the 'poles' of the shape (upper and lower points in shape depicted in panel (b) of figure 1), and the remaining ten pentagonal carbon rings are arranged around an 'equator' of the shape, in the polygon vertices of two parallel large pentagons rotated with respect to each other by an angle of $\pi/5$ (the vertices of one of those pentagons are denoted by points $P_1, \ldots, P_5$ in figure 1). The shapes can be uniquely characterized by the lengths of two vectors, $\mathbf{A}_1$ and $\mathbf{B}$, since $|\mathbf{A}_1| = |\mathbf{A}_2|$ (see figure 1). The lengths are integer multiples of the distance
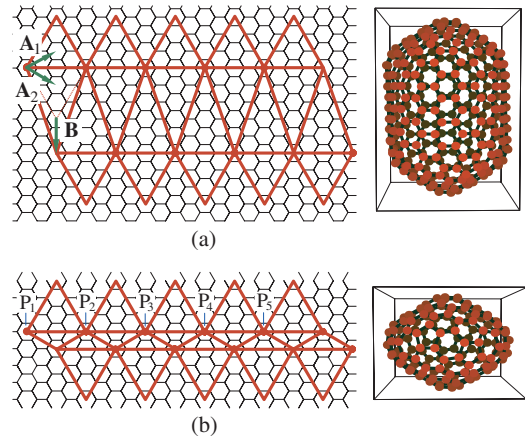

(a)

(b)

Figure 1. Geometric construction of the 'armchair' shapes of interest. The shape is cut out from the graphene plane and folded in an elongated (shape in panel (a)) or contracted (shape in panel (b)) or regular (not shown) icosahedron. Note that the points $P_1, \ldots, P_5$ (panel (b)) are situated in polygon vertices of a (large) pentagon once the shape is folded.

between the centres of neighbouring carbon hexagonal rings, i.e.

$$|\mathbf{A}_1| = |\mathbf{A}_2| = md,$$
$$|\mathbf{B}| = nd, \tag{1}$$
$$d = a\sqrt{3}$$

where a is the nearest neighbour C–C distance in graphite. I shall adopt the convention that negative values of n correspond to contracted shapes, so that the shapes in figure 1 can be described by ($m = 2, n = 2$) (elongated icosahedron) and ($m = 2, n = -2$) (contracted icosahedron). The (regular) icosahedral fullerenes are obtained for $n = 0$. The condition that has to be fulfilled by m and n integers is $n \geqslant -m$. For $n \gg m$, the construction results in capped armchair ($5m, 5m$) single-wall carbon nanotubes and this is the reason for giving the attribute 'armchair' to the chosen subset of shapes. The total number of carbon atoms (N) in the constructed shapes is

$$N = 60m^2 + 20mn. \tag{2}$$

Similar geometrical construction can be used to generate 'zigzag' or chiral (helical) shapes [18]. However, as the main intention of this work is in application of a continuum elasticity theory, the precise structure and atomic symmetry of the shape is of no importance, and only its shape matters in this respect. It should be noted here that the construction results in *single-shell* or *single-wall* carbon shapes/molecules. All the effects that are specific to multishell structures, in particular van der Waals interaction between the different shells, are not treated in this work. For the application of the continuum elasticity theory in the presence of van der Waals interactions and/or a surrounding elastic medium see e.g. [19, 20].

3. Finding the minimum-energy shapes

The mathematically constructed folded polyhedra will not represent the minimum energy shapes. Carbon atoms in a minimum-energy structure should be relaxed so that the
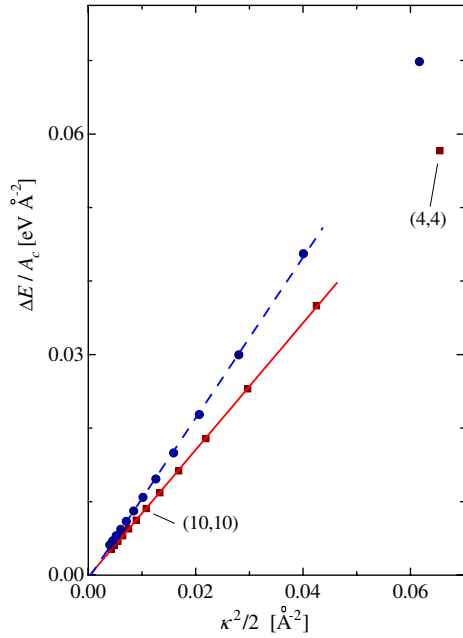
Figure 2. Excess energy per unit area as a function of squared cylinder (armchair carbon nanotube) curvature for the Tersoff potential [23] (circles) and the Brenner potential [22] (squares). The results for (4, 4) and (10, 10) armchair carbon nanotubes in this graph are denoted.

nearest-neighbour C–C distances and bond angles are close to their optimum value energywise. To account for these effects, one should have a reliable description of the energetics of carbon bonding. In this work, the C–C interactions are modelled using a relatively recent second-generation reactive empirical bond order potential by Brenner *et al* [22]. In this model, the potential energy (E_b) of a carbon structure is given by

$$E_b = \sum_i \sum_{j>i} \left[V^R(r_{ij}) - b_{ij} V^A(r_{ij}) \right], \qquad (3)$$

where r_{ij} is the distance between nearest-neighbour atoms i and j, V^R and V^A are pair-additive repulsive and attractive attractions, respectively, and b_{ij} is the bond order between atoms i and j that approximately accounts for the anisotropy of C–C bonding and for the many-body character of C–C interactions by including effectively the three-body contributions to E_b. The detailed description of the potential, together with all relevant parameters can be found in [22]. Similar potential models have been successfully employed in previous research of carbon structures (see e.g. [16, 17]).

The geometrically constructed, folded shape is used as the initial guess of the structure. The local minimum of E_b in the configurational space spanned by coordinates of all carbon atoms is found using the conjugate gradient technique described in [21]. The conjugate gradient technique optimizes all the coordinates at once, proceeding through a sequence of steps along the 'noninterfering' or 'conjugate' direction in the configurational space, so that a minimization along a particular direction does not spoil the effect of minimization in other conjugate directions. Similar procedures have been used for the same purposes in [12–14].

4. Energies of shapes and considerations based on elasticity theory

4.1. Infinitely long carbon cylinders (non-capped carbon nanotubes)

Conceptually the simplest shape that can be constructed from the graphene plane is the open-ended (non-capped) carbon nanotube. It does not result from the construction described in section 2, but will be examined first to enable a simple insight into the application of elasticity theory to the shapes of interest. I shall consider infinitely long single-walled armchair carbon nanotubes. The energetics of such shapes can be studied by applying the (one-dimensional) periodic boundary conditions to the carbon-nanotube unit cell (ring or several rings of atoms), so that the effective number of independent coordinates that have to be optimized with respect to total energy of the nanotube is relatively small. Figure 2 displays the energy of infinite, armchair-type carbon cylinders as a function of the squared cylinder curvature given by $\kappa = 1/\langle R_{cyl} \rangle$. The mean radius of the cylinder, $\langle R_{cyl} \rangle$, was calculated from the relaxed atomic coordinates as

$$\langle R_{cyl} \rangle = \frac{\sum_i \sqrt{x_i^2 + y_i^2}}{N}, \qquad (4)$$

where N is the total number of atoms in the unit cell, $\mathbf{r}_i = (x_i, y_i, z_i)$ is the position vector of the ith carbon atom and the cylinder axis coincides with the z-axis. The cylinder radius calculated from equation (4) is always very close to the analytical prediction for tube radius, $R = a/\{2 \sin[\pi/(3m)]\}$. For example, for (10, 10) carbon nanotubes, equation (4) and the numerically calculated values of $\mathbf{r}_i$ yield a nanotube radius of 6.802 Å, while the analytical prediction is 6.794 Å. The agreement becomes slightly worse with a decrease in the nanotube radius. The energies displayed in figure 2 are in fact excess energies *per unit area* of the structure (denoted by A_c; $A_c = 3a^2\sqrt{3}/4$) and were calculated as

$$\frac{\Delta E}{A_c} = (E_{cylinder}^{per\ atom} - E_{graphene}^{per\ atom}) \frac{4}{3a^2\sqrt{3}}, \qquad (5)$$

where $E_{cylinder}^{per\ atom}$ and $E_{graphene}^{per\ atom}$ are the energies *per atom* in the cylinder and in the graphene plane, respectively. The calculations were carried out for two versions of the carbon–carbon potential, which obviously predict different slopes of the dependence of the excess energy on squared curvature, but note that both curves are *linear* up to very large curvatures, i.e. small radii of carbon nanotubes. Calculations with the early Tersoff potential [23] predict that somewhat larger energies are required to bend a piece of graphene plane in a cylinder with respect to those obtained by using the latest Brenner potential [22]. For the energy per unit atom in the graphene plane the two potentials predict $E_{graphene}^{per\ atom} = -7.395\,52$ eV (Tersoff's potential) and $E_{graphene}^{per\ atom} = -7.394\,94$ eV (Brenner's potential). A more important difference between the two potentials is in the equilibrium C–C bond lengths they predict ($a = 1.4605$ Å and $a = 1.4204$ Å for the Tersoff and Brenner potentials, respectively). The slopes of the lines shown in figure 2 (c_0) were obtained from fitting the calculated results pertaining to (5, 5), (6, 6), ..., (16, 16) carbon nanotubes, and

for the Brenner and the Tersoff potential they are 0.863 ± 0.003 eV and 1.093 ± 0.006 eV, respectively (Tersoff obtained $c_0 = 1.02$ eV in [16]).

The demonstrated linear dependence of the excess energy per unit area on squared (mean) curvature can be easily understood from the examination of the geometry of a bent network of graphene bonds. Consider a piece of graphene plane bent on a large cylinder of radius $R \gg a$. The most important change in the energetics of the carbon network is due to a *change in angles between the bonds*, while the bond lengths remain the same as in graphene. Only the bond order term, b_{ij}, depends on the angles between bonds (see equation (3) and [22, 23]). By purely geometrical considerations it is easy to derive how the angles between the bonds change when the graphene plane is rolled onto a cylinder. If one assumes the plane to be inextensional, and considers large cylinder radii ($a/R \ll 1$), the change in energy per ith atom is given by

$$\Delta E_i = \frac{1}{2} V^{\mathrm{A}}(a) \left[\frac{\partial b_{ij}}{\partial \cos(\theta_{ijk})} \right]_{-1/2} \left(\frac{3a}{4R} \right)^2, \quad (6)$$

which can also be written as

$$\frac{\Delta E}{A_c} = \frac{1}{2} V^{\mathrm{A}}(a) \left[\frac{\partial b_{ij}}{\partial \theta_{ijk}} \right]_{2\pi/3} \frac{\kappa^2}{2}, \quad (7)$$

where j is the index of one of the three nearest neighbours of the ith atom, $k \neq j$ is either of the remaining two neighbours of i and the angle between the i–j and i–k bonds is θ_{ijk}.[1] The explicitly written factor of $1/2$ is a consequence of the fact that the energy in the Tersoff–Brenner potentials is situated in C–C bonds, and that each bond is shared by *two* atoms. Equation (7) is most easily derived by considering armchair or zigzag carbon nanotubes, since in these cases one of the bonds is either parallel (zigzag) or perpendicular (armchair) to the cylinder axis, but for $a/R \ll 1$, the relation also holds for helical nanotubes; i.e., for small curvatures the bending energies do not depend on the symmetry of the carbon nanotube. Note again that the analytical expression (7) accounts for the excess energy only in the limit of small curvatures κ, i.e. for radii of curvature that are large with respect to the graphene lattice constant.

Equation (7) shows that the excess energy per unit area is proportional to the squared curvature, in accordance with the results produced by calculations displayed in figure 2 (note, however, that only a curvature along one direction is accounted for by equation (7), which is sufficient for a cylindrical surface). It furthermore predicts that the slope of this dependence is given by the properties of the interatomic potential (intriguingly, the factor of proportionality does not depend on the form of the repulsive part of the potential for the class of bond order potentials given in [22, 23]). The slope c_0 can be easily read out from equation (7), and is calculated to be $c_0 = 0.8301$ and 1.0152 eV for Brenner's and Tersoff's potentials respectively. This is fairly close to the slopes obtained numerically. The small difference can be attributed to the fact that equation (7) is valid only for small

---

[1] The bond order function b_{ij} includes summation over k, the remaining two neighbours of i, $k \neq j$ (see [22, 23]). When evaluating the derivative in equation (7), all the indices (i, j, k) are to be considered as fixed, but the summation over k in b_{ij} of course remains.

curvatures (or large radii, $a/R \ll 1$), i.e. it includes only the lowest order contribution of curvature (quadratic). For tubes of small radii, higher order terms are expected to be of importance. In fact, if one restricts the linear fit in figure 2 to smaller curvatures (from (12, 12) to (16, 16) nanotubes, $a/R < 0.175$) one finds that the slopes are 0.839 and 1.036 eV, which is in significantly better agreement with the prediction of equation (7). Note that for (5, 5) nanotubes, $a/R = 0.414$, which means that the tubes of such small radii are already in the region where condition $a/R \ll 1$ does not hold, and the predictions of equation (7) are not expected to be very accurate.

The key conclusion of this subsection is that the excess energy per carbon atom (ΔE) of an infinitely long carbon cylinder can be reliably estimated from

$$\frac{\Delta E}{A_c} = c_0 \frac{\kappa^2}{2}, \quad (8)$$

where c_0 is the elastic constant of the graphene plane related to the energetics of its bending (the bending rigidity), which, for infinitesimal curvatures, can be calculated from the knowledge of the interatomic interactions in graphene as in equation (7). This equation holds irrespective of the details of the interatomic interactions, which only change the *value* of c_0 and not the *functional dependence* displayed in equation (8), which was illustrated by the examination of energetics predicted by two different models of C–C interactions [22, 23]. Equation (8) can also be understood without reference to the atomic structure of the carbon nanotube by interpreting its left-hand side as the bending energy per unit area of the material.

4.2. Icosahedral fullerenes

Icosahedral fullerenes are an $(m, n = 0)$ subset of shapes considered in section 2. They are more complex than the infinite carbon nanotubes from the standpoint of elasticity theory since they contain 12 pentagonal disclinations situated at vertices of an icosahedron. The excess energy of icosahedral fullerene relative to a piece of infinite graphene sheet with the same number of atoms is thus a result of both bending (and possibly stretching) of the sheet *and* the energy required to create disclinations. In order to calculate the bending contribution to the energy, one should have some information on the geometry of the minimal energy shape of the icosahedral fullerene. The pentagonal disclination can be constructed in a graphene plane, starting from the centre of a hexagon, and cutting the plane in two directions that make an angle of 60°— these cuts can be easily seen in the geometrical constructions in figure 1. The smaller, cut-out piece of graphene is discarded and the remaining (larger) piece of graphene is then folded to rejoin the edges of the cut. The shape of minimal energy that the remaining piece of graphene adopts is a cone, since it costs less energy to bend the C–C bonds than to stretch them (it is convenient to imagine a circular piece of graphene plane with a hexagon in its centre). The shape will in fact be a truncated cone (or a *conical frustum*), since the pentagonal ring at the top of the cone will be flat and parallel to the larger base of the cone. The precise description of the shape depends on the values of two-dimensional Young's modulus and bending rigidity. For materials like graphene (whose

stretching requires much more energy than bending), the conical frustum is an excellent approximation of the minimal-energy shape. From purely geometrical considerations, the half-angle of the cone is easily shown to be $\sin^{-1}(5/6)$. Shapes of crystalline, hexagonally coordinated membranes with pentagonal disclinations have been studied in [14], and many of the features discussed there also apply to the case of graphene. The icosahedral fullerene is a bit more complicated than a single cone since it contains *12* pentagonal carbon rings. It seems plausible that the fullerene shape should be well described by the *union* of 12 truncated cones. The radius of the larger base of a particular cone is restricted by the presence of other cones. To illustrate these geometrical considerations, in figure 3 the shape of the ($m = 4, n = 0$) icosahedral fullerene is displayed (left column of images), which is in a minimum of total energy, obtained numerically as discussed in section 3. The images in the right column of figure 3 display a union of 12 cones with half-angles of $\sin^{-1}(5/6)$ whose larger bases just touch. Note that this geometrical construction is an excellent approximation to the *calculated* minimal energy shape. Its small drawback is that its total area (without inclusion of the areas of the larger bases of the cones) is smaller than the total area of the fullerene shape, which is manifested in figure 3 by the appearance of 'holes'. Note also that the regions where these holes appear are almost flat in the numerically calculated minimal energy shape of the fullerene, and their contribution to the bending energy should thus be small.

Having such a good representation of the shape, it is possible to directly proceed to the calculation of its bending energy. In the continuum elastic theory of membranes [24], the bending energy (H_b) is represented as

$$H_b = \tfrac{1}{2} \int_{\text{Surface}} dS \left(c_0 \kappa^2 + 2c_G \gamma \right), \tag{9}$$

where c_0 is the bending rigidity discussed in the previous subsection, c_G is the Gaussian rigidity, dS is the infinitesimal element of the shape surface and κ and γ are the mean and Gaussian curvature of the surface, respectively (if R_1 and R_2 are the principal radii of curvature, $\kappa = R_1^{-1} + R_2^{-1}$, and $\gamma = (R_1 R_2)^{-1}$). Note that for a cylindrical surface $\gamma = 0$ and $\kappa = 1/R_{\text{cyl}}$ ($R_1 = R_{\text{cyl}}, R_2 = \infty$) at every point of the surface, and the total bending energy integrates to $H_b/A = c_0 \kappa^2/2$, where A is the total area of the cylinder (without bases). This is in agreement with equation (8). For conical surfaces, the Gaussian curvatures are also zero everywhere, so the total bending energy of the approximated fullerene shape will depend only on c_0. Integrating equation (9) over the surface of a cone whose half-angle is β, one finds that the bending energy of a cone (H_b^c) is

$$H_b^c = \frac{\cos^2 \beta}{\sin \beta} \pi c_0 \ln \left(r_{\text{max}}/r_{\text{min}} \right), \tag{10}$$

which for the cones with $\beta = \sin^{-1}(5/6)$ yields [16]

$$H_b^c = \frac{11\pi}{30} c_0 \ln \left(r_{\text{max}}/r_{\text{min}} \right), \tag{11}$$

where the meaning of r_{min} and r_{max} is illustrated in panel (c) of figure 3—these are the distances of the upper and lower bases of the conical frustum from the cone apex measured along the
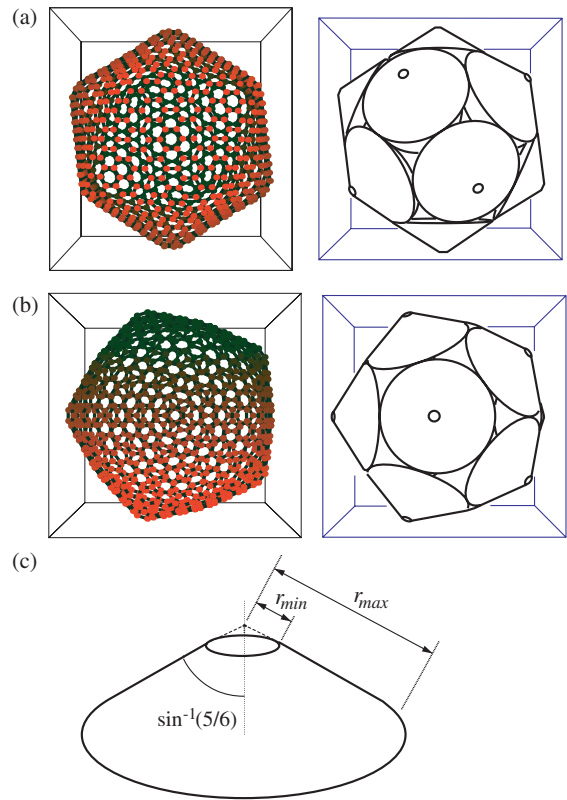
Figure 3. (a) Equilibrated, minimal energy ($m = 4, n = 0$) shape (left) and its approximation by 12 conical frusta whose smaller base centres are situated at the vertices of an icosahedron (right). (b) The same as in panel (a), only viewed from a different point. (c) The elementary building block of the shapes shown in the right columns of panels (a) and (b)—a conical frustum whose half-angle is $\sin^{-1}(5/6)$. The quantities relevant to equation (11) are denoted.

cone face. The value of r_{min} can be easily evaluated due to the fact that the smaller base of the frustum is a pentagon of carbon atoms. There is some ambiguity, however, since the pentagon is to be approximated by a circle. If the *circumradius* of the pentagon is identified with the radius of the smaller base of the cone, one obtains that $r_{\text{min}} = 3a\sqrt{50 + 10\sqrt{5}}/25 \approx 1.021a$, which is the upper bound for r_{min}. The identification of the radius of the smaller base of the cone with the *inradius* of the pentagon yields $r_{\text{min}} = 3a\sqrt{25 + 10\sqrt{5}}/25 \approx 0.826a$, which is the lower bound for r_{min}. In any case, $r_{\text{min}} = fa$, where f is a numerical factor between 0.826 and 1.021. The value of r_{max} is half of the shortest distance between the two apices of the neighbouring cones measured along the cone faces. From figures 1 and 3, one finds that $r_{\text{max}} = 3(m - 2)a/2 + r_{\text{min}}$, and by using equation (2) one obtains that

$$\frac{r_{\text{max}}}{r_{\text{min}}} = \frac{3}{2f} \sqrt{\frac{N}{60}} + \frac{f - 1}{f}. \tag{12}$$

It is obviously quite convenient to choose $f = 1$, closer to the upper bound for r_{min}, so that the total excess energy of the icosahedral fullerene can be written as

$$\Delta E(N) = 12 \left[\lambda_5 + \frac{11\pi}{60} c_0 \ln \left(\frac{N}{60} \right) + \frac{11\pi}{30} c_0 \ln \left(\frac{3}{2} \right) \right] + E_{\text{holes}}. \tag{13}$$

The multiplicative factor of 12 in the above equation is due to the sum of the energies of 12 cones that make the shape surface, and λ_5 is the *core energy* of the pentagonal disclination, which contains the local effects associated with the atomic structure of the carbon pentagon and its immediate neighbourhood. The contribution of the part of the fullerene surface that was not covered by the union of cones to the total energy was denoted by E_{holes}. Note that this quantity should represent a quite small correction to the total energy (see figure 3) and is not expected to depend strongly on N, since the area of the 'holes' is proportional to N, while their mean curvature is approximately proportional to $1/\sqrt{N}$ (inverse radius of the fullerene, see equation (9)). Although one could easily invent a nice geometrical model to estimate this contribution, it is possible to proceed further by noting that equation (13) can also be written as

$$\Delta E(N) = \Delta E(C_{60}) + \left[\frac{11\pi}{5} c_0 \ln \left(\frac{N}{60} \right) \right], \qquad (14)$$

where $\Delta E(C_{60})$ is the total excess energy of C_{60} for which the calculation with the Brenner potential predicts $\Delta E(C_{60}) = 26.744$ eV. Figure 4 displays the results of numerical minimization of total energy of icosahedral fullerenes together with the prediction of equation (14) with $c_0 = 0.863$ eV taken from the analysis of infinite carbon cylinders. It seems more sensible to choose this value of c_0 rather than the one predicted by equation (7), which is appropriate for small curvatures, since close to the smaller bases of the truncated cones condition $a/R \ll 1$, where R is the radius of curvature, is not fulfilled. Thus, a usage of a somewhat larger value of c_0 obtained from the numerical analysis of an infinite carbon cylinder should approximately account for the contribution of terms like $(a/R)^p$, $p > 2$, to the bending energy of the shapes studied. Note, however, that the (infinitesimal) analytical value of c_0 (0.83 eV) and the one obtained from the study of infinite carbon cylinders (0.863 eV) are quite similar, and one could also chose to work with the analytical value of c_0 with comparable success (see below).

It can be seen in figure 4 that the agreement between the calculated values and those predicted by equation (14) is excellent (note that there are *no fit parameters*). Very small deviations can be mostly attributed to the fact that the regions around the larger bases of the cone are constrained by the continuity of the fullerene surface, and deviation from the cone shape is thus expected. It is to a certain extent surprising that the predictions of equation (14) are so precise, especially concerning the fact that the excess energy of C_{60} figures in it as a parameter. Buckminsterfullerene is certainly not expected to be reliably described by the elasticity theory, since there are no atoms on the cone faces, only C–C bonds. Yet, the elasticity theory results maintain their meaning down to fullerenes of very small sizes and small number of atoms. By examining the energies of individual atoms in the icosahedral fullerenes it is possible to proceed a bit further and to estimate the value of the core energy, λ_5. For example, in $(m = 4, n = 0)$ fullerene shown in figure 3, the energies of atoms in pentagonal rings are -6.959 eV, while atoms situated in hexagonal carbon rings have energies of about -7.38 eV, depending on their position (see equation (3)). The energies of atoms in pentagonal rings do not change significantly with increasing the size of
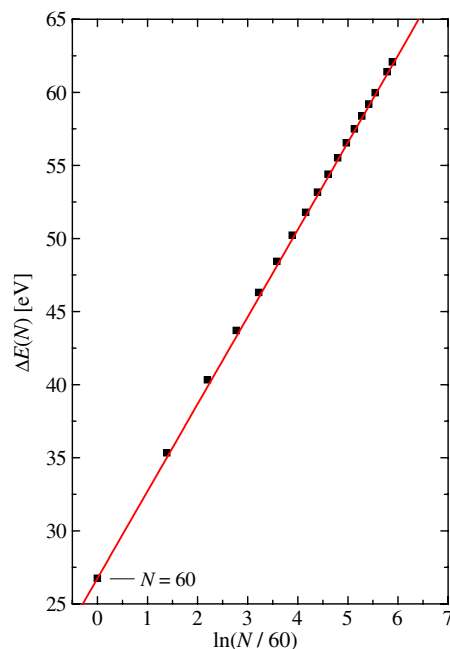

Figure 4. Numerically calculated excess energies of icosahedral fullerenes (squares) and the prediction of equation (14) (line).

the fullerene, which is a consequence of the *local* nature of this energy. All this suggests that $\lambda_5 = 5[-6.9587 - (-7.3949)]$ eV $= 2.18$ eV, where -7.3949 eV is the energy per atom in the infinite graphene plane, predicted by the Brenner potential. Equation (14) does not depend (formally) on this quantity, but it can be calculated from equation (13), which yields $\lambda_5^{elast} = 1.83$ eV (E_{holes} was set to zero), in a quite nice agreement with the number obtained from the detailed atomic description of the icosahedral fullerenes, especially in view of all the details involved in the approximation of the fullerene shape. This also confirms that E_{holes} is indeed a negligible part of the total energy.

4.3. Capped carbon nanotubes, elongated icosahedral fullerenes

Using the same reasoning as outlined in the previous subsection, it is easy to construct an approximate shape of the elongated icosahedral fullerene ($n \neq 0$). It can be approximated by the union of 12 conical frusta *and* a cylinder whose length is $na\sqrt{3}$, and radius $15ma/(2\pi)$ (a finite-length piece of armchair $(5m, 5m)$ carbon nanotube). The excess elastic energy can be thus written as

$$\Delta E(m, n) = 12 \left[\lambda_5 + \frac{11\pi c_0}{30} \ln \left(\frac{3m}{2} \right) \right] + \frac{2\pi^2 c_0}{5\sqrt{3}} \frac{n}{m} + E_{holes}, \tag{15}$$

which could also be parameterized by the total number of atoms, N, and n. The first term in the expression for energy in equation (15) is the sum of the local and bending energies associated with the 12 equal pentagonal disclinations (conical frusta), and the second one corresponds to the bending energy of the finite length cylinder. The third term is again the energy associated with the 'holes' in the geometrical construction,
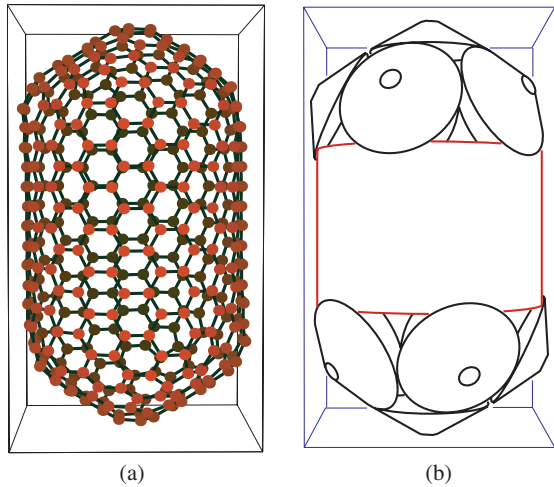
Figure 5. (a) Numerically calculated equilibrium shape of $(m = 2, n = 4)$ elongated icosahedral fullerene. (b) Approximation of shape using geometrical construction leading to equation (15).

Figure 6. (a) Excess energies of elongated icosahedral fullerenes (capped carbon nanotubes) as a function of elongation number (n) with m as a parameter of the curves. Full symbols correspond to numerically calculated excess energies, while lines correspond to the predictions of elasticity theory in equation (16). (b) The same data as in panel (a) with the roles of m and n numbers interchanged.

as discussed in the previous subsection. Note that for $n = 0$ equation (15) reduces to equation (13). Although the geometrical construction yielding equation (15) is quite simple, it has a small drawback in that the areas of the cones and of the cylinder in between them overlap to a small extent. Angles between the surfaces of the cones and the cylinder at the points in which the entities nearly touch are small but nonvanishing, which is another drawback of the proposed construction. More elaborate constructions are possible, but are not needed (figure 6). Equation (15) can be approximated by

$$\Delta E(m, n) = \Delta E(C_{60}) + \left[\frac{22\pi}{5} c_0 \ln(m) + \frac{2\pi^2 c_0}{5\sqrt{3}} \frac{n}{m} \right],$$
(16)

which simply states that the excess energy of the shape is equal to the sum of the excess energy of the icosahedral fullerene and the bending energy of the cylinder inserted in between its two 'halves' (see figure 5). This equation is, however, an approximation, since it is based on the assumption that the excess energies associated with the holes in the geometrical constructions are the same for the icosahedral fullerene and the elongated icosahedral fullerene, which is not exactly the case (compare figures 5 and 3). It furthermore contains an assumption that the elastic energies of holes do not depend on m and n integers characterizing the structure. Nevertheless, an excellent account of the numerical data is obtained, which can be seen from figure 6. Note again that the analytical results presented in figure 6 represent the predictions of the elasticity theory *without* fit parameters.

4.4. Contracted icosahedral fullerenes

The contracted icosahedral fullerenes are more complicated than the shapes considered thus far. Construction of their geometrical approximation is not simple mostly due to specific geometrical constraints that the ten pentagonal disclinations situated around the equator of the shape are subjected to. When n vanishes, the area around each of the disclinations is well
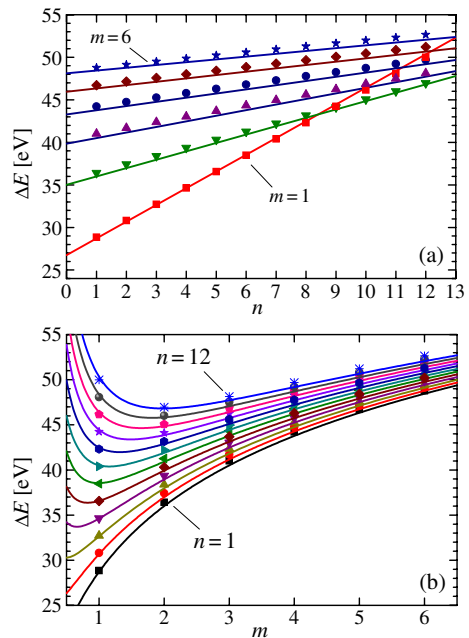
represented by a cone with an angle of $2\sin^{-1}(5/6)$, which was clearly demonstrated in section 4.2. When n decreases (i.e. increases in absolute value), the two large pentagons parallel to the shape equator whose vertices coincide with five pentagonal disclinations (see figure 1) approach each other. This constrains the shape of the area around these pentagonal disclinations. As the cone was such a useful approximation of the area around pentagonal disclinations for shapes studied in sections 4.2 and 4.3, it seems reasonable to try to describe the contracted icosahedral fullerenes also as union of cones, ten (those arranged around the equator of the shape) of which belong to one category, and two (the ones at the two poles of the shape) to another. The two cones at the poles are easily constructed as in sections 4.2 and 4.3—these have the angles of $2\sin^{-1}(5/6)$. The area around ten remaining disclinations is dominated by two opposing geometrical constraints. As n decreases, the angle subtended by a line that connects a particular disclination (point A in panel (b) of figure 7) and the one at the closest pole (point B) and a line that connects the disclination with the midpoint of a line drawn between the two nearest disclinations in the neighbouring pentagonal ring of disclinations (point C) also decreases—this angle is denoted by α_1 in panel (b) of figure 7. On the other hand, the angles that are subtended by the lines $\overline{DA}$ and $\overline{AE}$ or $\overline{FA}$ and $\overline{AG}$ (see figure 7) *increase* when n decreases. It is thus clear that the area around the disclination cannot be represented by a *single* cone. Nevertheless, it seems reasonable to approximate this area by a union of pieces of surfaces of two cones, each of them satisfying one of the two opposing geometrical constraints.

The angle of one of the cones is about α_1, which is given by

$$\alpha_1(n) = \cos^{-1}\left[\frac{1}{2\sin(\pi/5)}\right] + \cos^{-1}\left[\frac{\sqrt{3}m\tan(\pi/10)}{3m-2n}\right]. \tag{17}$$

The angle of the second cone (α_2) that is searched for is larger than α_1, and the contribution of this half-cone to the total elastic energy of the area surrounding the disclination is thus smaller (see equation (10)). Nevertheless, the second cone is important since it contains a part of the total area surrounding the disclination, thus reducing the area available to the cone with angle α_1. When $n = 0$, both α_1 and α_2 angles should be $2\sin^{-1}(5/6)$. Note that when n decreases angle α_2 changes in a significantly smaller range than α_1, since it is importantly constrained by the fixed angle between lines $\overline{DA}$ and $\overline{AH}$ (see figure 7). Thus, I shall neglect the change of α_2 with n and set it to a constant

$$\begin{aligned}
\alpha_2 &= 4\sin^{-1}(5/6) - \alpha_1(n=0) \\
&= 4\sin^{-1}(5/6) - \cos^{-1}\left[\frac{1}{\sin(\pi/5)}\right] - \cos^{-1}\left[\tan(\pi/10)\right] \\
&\approx 2.04\sin^{-1}(5/6),
\end{aligned} \tag{18}$$

which is obviously quite close to $2\sin^{-1}(5/6)$, as it should be, and which was chosen so that $\alpha_2 + \alpha_1(n=0) = 4\sin^{-1}(5/6)$, since I am further going to assume that each of the two cones takes exactly a half of the total area available to the disclination. Together with the choice for α_2 in equation (18), this assumption will yield the elastic disclination energy in the limit when $n = 0$ equal to that characteristic of icosahedral fullerenes studied in section 4.2. Note that the *axes* of the two cones do not need to be identical—the two pieces of the conical surfaces can be rotated with respect to each other at will. It is also irrelevant how the particular cone (half) surface is constructed as long as the pieces of it are bounded by the arcs of the two bases subtending the same angle from the cone axis and the two lines (along the cone face) that connect the arc ends in the upper and lower base. Thus, there is a significant freedom in constructing a shape around the disclination, but for all of the thus constructed shapes the buckling energies are equal. Note also that for $n \neq 0$ points D, B, H and E do not lie in a plane. The proposed construction is admittedly rather approximate. For example, one could object that the fractions of the total area belonging to each of the two cones should also (at least slightly) change with n. Nevertheless, the construction accounts for *most important* geometrical constraints imposed on the area around pentagonal disclinations situated around the equator of the shape due to the presence of neighbouring disclinations. The exact answers to all of the objections regarding the proposed construction that could be easily put forth would require a solution of the nonlinear problem in the theory of elasticity, which is not the aim of this study—the aim is to obtain a simple insight into the energetics of the shapes using the simplest possible application of the elasticity theory, and to obtain, preferably analytic, expressions for the excess energies of such shapes.

Following the reasoning presented in the previous paragraph and using equation (10) for the calculation of bending energy of a cone with arbitrary half-angle, the total excess energy of the proposed geometrical approximation to
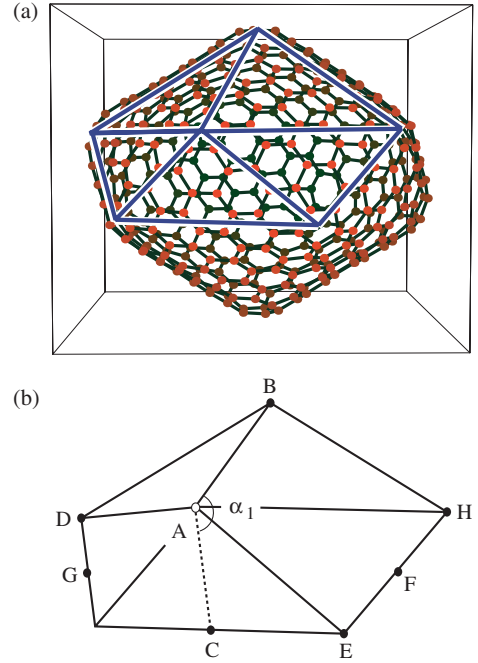

(a)

(b)

Figure 7. (a) Equilibrium shape of ($m = 3$, $n = -2$) contracted icosahedral fullerene. The characteristic pyramid-like shape is denoted by full lines. (b) The pyramid-like shape with denotations discussed in the text.

the contracted icosahedral shapes is

$$\Delta E(m,n) = 12\lambda_5 + 2E_{\text{pole}}(m,n) + 10E_{\text{equator}}(m,n) + E_{\text{holes}}, \tag{19}$$

where

$$E_{\text{pole}} = \frac{11c_0\pi}{30}\ln(3m-q), \tag{20}$$

$$E_{\text{equator}} = \frac{c_0\pi}{2}\ln(q)\left\{\frac{\cos^2[\alpha_1(n)/2]}{\sin[\alpha_1(n)/2]} + \frac{\cos^2(\alpha_2/2)}{\sin(\alpha_2/2)}\right\}, \tag{21}$$

and

$$q = \frac{\sqrt{9m^2 + 3(3m-2n)^2}}{4}. \tag{22}$$

The last parameter (q) is simply a half of the distance (in units of a) between the two nearest neighbouring disclinations situated at different pentagonal rings of disclinations around the equator of the shape (points A and E in figure 7).

Numerically calculated excess energies of the shapes and the predictions of equation (19) are shown in figure 8 and denoted by symbols and lines, respectively. In evaluating equation (19), E_{holes} was set to zero, $\lambda_5 = 1.83$ eV was taken from the analysis of icosahedral fullerenes in section 4.2 and $c_0 = 0.863$ eV, as in the two previous subsections. Note again that there are no fitting parameters involved. The agreement of the predictions of the elasticity theory with the numerical results is striking. In spite of all the approximations involved in the geometrical construction of the equilibrium shape, equation (19) both qualitatively and quantitatively accounts for the numerical data. The largest disagreement is found for the smallest shapes ($m = 2$), but the curves correctly account for the appearance of a minimum in excess energies for some finite n (panel (a) of figure 8), and for the increase in excess
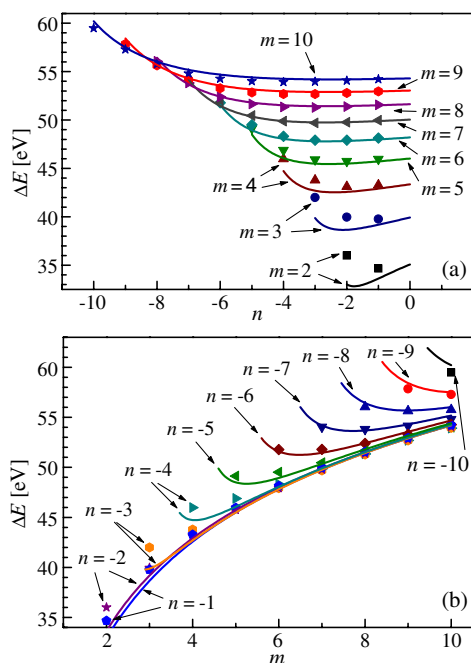
Figure 8. (a) Excess energies of contracted icosahedral fullerenes as a function of n with m as a parameter of the curves. Full symbols correspond to numerically calculated excess energies, while lines correspond to the predictions of equation (19). (b) The same data as in panel (a) with the roles of m and n numbers interchanged.

energies when $|n|$ becomes comparable to m. It is worth noting that although the number of atoms in $n = -m$ structures is smaller than in $(m, n = 0)$ structures (regular icosahedral fullerenes) by 20 mn (see equation (2)), the total excess energies are still significantly larger in such structures, which is a consequence of an energetically unfavourable geometrical position occupied by the ten disclinations around the equator of the shape. This consideration can also explain the minimum in excess energies obtained for some n when m is fixed—as the elongation number n decreases, the number of atoms in the structure decreases, but the contribution to excess energy due to the ten disclinations around the equator increases. The combined consequences of these two effects lead to the appearance of a minimum in excess energy as a function of n. Of the three types of shapes studied, the contracted icosahedral fullerenes typically have the largest excess energies per atom. For example, the excess energy of $(m = 10, n = -10)$ contracted fullerene ($\Delta E = 59.47$ eV) that contains 4000 atoms is significantly *larger* than the excess energy of $(m = 9, n = 0)$ regular icosahedral fullerene ($\Delta E = 53.16$ eV) that contains a *larger* number of atoms ($N = 4860$).

5. Summary and conclusion

It has been shown that insight into the geometry of the equilibrium shapes can be extremely useful in estimating their (excess) energies. Such an approach does not require detailed description of the interatomic interactions characteristic of a shape or molecule in question; instead, it relies exclusively on the knowledge of elastic parameters of the material that the shape (shell) is made of. In the studies presented in this paper,

the parameters that were necessary for reliable estimation of energy were the local energy of a pentagonal ring of carbon atoms (λ_5), and the bending rigidity of a graphene plane (c_0). Both of these parameters derive from the quantum mechanical nature of bonding of atoms (see equation (7)) that make the shape. Surprisingly enough, it has been demonstrated that the application of the simplest theory of elasticity yields reliable results even for shapes made of a small number of atoms, i.e. in the regime where its applicability is not to be expected. For all of the shapes considered, knowledge of the two-dimensional Young's modulus of graphene [24] was not needed, which suggests that in such shapes almost all of the elastic energy is of the *bending* type, while the energies associated with stretching are negligible[2]. For shapes in which the geometrical constraints on the shape are strong (as in the case of contracted icosahedral fullerenes), the application of elasticity theory may be involved and complicated. Nevertheless, the identification of the constraints and their effects on the allowed shapes yields an additional insight into the energetics of the shapes and its behaviour within a certain class of shapes studied.

References

[1] Kroto H W, Heath J R, O'Brien S C, Curl R F and Smalley R E 1995 *Nature* **318** 162
[2] Ijima S 1991 *Nature* **354** 56
[3] Ge M and Sattler K 1994 *Chem. Phys. Lett.* **220** 192
[4] Krishnan A, Dujardin E, Treacy M M J, Hugdahl J, Lynum S and Ebbesen T W 1997 *Nature* **388** 451
[5] Smith B W, Monthioux M and Luzzi D E 1998 *Nature* **396** 323
[6] Han J, Globus A, Jaffe R and Deardorff G 1997 *Nanotechnology* **8** 95
[7] Hamada N 1993 *Mater. Sci. Eng.* B **19** 181
[8] Coluci V R, Galvao D S and Jorio A 2006 *Nanotechnology* **17** 617
[9] Vanderbilt D and Tersoff J 1992 *Phys. Rev. Lett.* **68** 511
[10] Fraenkel-Conrat H and Singer B 1999 *Phil. Trans. R. Soc. Lond.* B **354** 583
[11] Kroto H W and McKay K 1988 *Nature* **331** 328
[12] Lidmar J, Mirny L and Nelson D R 2003 *Phys. Rev.* E **68** 051910
[13] Nguyen T T, Bruinsma R F and Gelbart W M 2005 *Phys. Rev.* E **72** 051923
[14] Seung H S and Nelson D R 1988 *Phys. Rev.* A **38** 1005
[15] Baker T S, Olson N H and Fuller S D 1999 *Microbiol. Mol. Biol. Rev.* **63** 862
[16] Tersoff J 1992 *Phys. Rev.* B **46** 15546
[17] Robertson D H, Brenner D W and Mintmire J W 1992 *Phys. Rev.* B **45** 12592
[18] Terrones M, Terrones G and Terrones H 2002 *Struct. Chem.* **13** 373
[19] Ru C Q 2001 *J. Mech. Phys. Solids* **49** 1265
[20] He X Q, Kitipornchai S, Wang C M and Liew K M 2005 *Int. J. Solids Struct.* **42** 6032
[21] Hager W W and Zhang H 2005 *Siam J. Optim.* **16** 170
[22] Brenner D W, Shenderova O A, Harrison J A, Stuart S J, Ni B and Sinnott S B 2002 *J. Phys.: Condens. Matter* **14** 783
[23] Tersoff J 1989 *Phys. Rev.* B **39** 5566
[24] Landau L D and Lifshitz E M 2002 *Theory of Elasticity* (Oxford: Butterworth-Heinemann)
[25] Lobkovsky A F 1996 *Phys. Rev.* E **53** 3750
[26] Witten T A and Li H 1993 *Europhys. Lett.* **23** 51

---

[2] This, however, may change for extremely large fullerene molecules where the effects associated with the sharpening of the shape ridges may be of importance [25, 26].